On the size and shape of self-assembled micelles

Peter H. Nelson, Gregory C. Rutledge, and T. Alan Hatton[a)]
Department of Chemical Engineering, Massachusetts Institute of Technology, Cambridge, Massachusetts 02139

(Received 9 June 1997; accepted 16 September 1997)

Equilibrium size and shape distributions of self-assembled micelles are investigated using lattice Monte Carlo simulation techniques. The micellar size distributions are shown to include a Gaussian peak of spherical micelles, in combination with an exponential tail of cylindrical micelles. © *1997 American Institute of Physics.* [S0021-9606(97)50248-0]

INTRODUCTION

Recently, there have been a number of studies of micelle formation using computer simulations of coarse grained bead-type models.[1–15] The motivation for using simplified models is that the computational requirements for equilibrating more realistic models are too demanding, at present, primarily due to the long time scales involved in self-assembling systems. In addition, a relatively large system size is required to accommodate even a modest number of micelles. Fortunately, there appear to be universal properties of aggregate formation and structure which are similar for many different surfactant systems.[10] It is these properties which the simplified models are intended to investigate. The very simplicity of the model can be an asset in determining which microscopic properties are responsible for observed aggregate characteristics.

In previous simulations,[9,15] the size distributions of relatively small micelles with aggregation numbers less than 100 were modeled using an empirical approach based on the dilute solution excess chemical potential determined from the measured size distribution. In this paper, we investigate distributions of equilibrium aggregates of up to 500 surfactants and fit their size distributions to widely accepted phenomenological theories which assume the micelles have spherical and cylindrical shapes.

In determining the size of the system to be simulated, Larson[3] has noted that it is the number of aggregates in the simulated system that is of importance in determining finite size effects. As a result we chose a small surfactant occupying four lattice sites and a large lattice size. Recent results[9] are consistent with the relatively smooth single-peaked micellar size distributions reported here. In what follows, we compare our results with the simple thermodynamic models which assume spherical and cylindrical micellar shape.

THE SIMULATED SYSTEM

The simulations reported here were conducted on a face centered cubic lattice with periodic boundary conditions implemented along the three lattice directions in the usual way. The surfactants used here occupy four lattice sites and are linear symmetric H_2T_2 molecules comprising two ''hydrophilic'' head beads (H) and two ''hydrophobic'' tail beads (T). The remainder of the lattice is filled with ''water'' beads (W). This provides a simple Flory–Huggins-type model[16] for the system. The pairwise interaction energies were chosen to be $\epsilon_{HH}=\epsilon_{TT}=\epsilon_{WW}=\epsilon_{HW}=0$ and $\epsilon_{HT}=\epsilon_{WT}=\epsilon$, so that the head and water beads interact as if they were identical to each other.[1–9] With these values the lattice energy can be thought of as an excess energy of mixing. Hence, the system is characterized by a single χ parameter

$$\chi=\frac{z}{T'};\quad T'=\frac{k_BT}{\epsilon},$$

where $z=12$ is the coordination number of the lattice, T' is a scaled temperature, k_B is the Boltzmann constant and T is the temperature.

The simulated surfactants are not directly comparable to any real surfactant systems, but qualitative comparison with short-length nonionic surfactants is justified. For example, the hydrophobic tail may be compared with an alkane chain of up to about C_{20} length if each bead is considered to represent one Kuhn segment length. (A more direct physical interpretation of the hydrophobic tail is of a rigid ''rod'' formed by two moieties connected by a fixed-length bond.)

A form of the general reptation algorithm was used for moving the surfactants through the lattice. Details of the bead algorithm used here are described elsewhere.[17,18] Standard Metropolis sampling techniques were used to determine whether a motion attempt should be accepted.

TEMPERATURE DEPENDENCE

In order to investigate the temperature dependence of the system and to select a temperature for the main simulation run, we ran a number of simulations on much smaller lattices ($20\times20\times20$) at the same volume fraction (7.5%) as the main simulation. On this smaller lattice there were only 150 surfactants in the system. Figure 1 shows the resulting size distributions of the micelles for scaled temperatures ranging from $T'=2.0$ to $T'=2.4$. Each point on the graph represents an integer aggregation number; no smoothing of the distribution was performed. The definition of an aggregate (micelle) is[1–9] a collection of surfactant molecules whose tail blocks are touching each other. The values plotted in Fig. 1 are the volume fraction of surfactant at a given state of ag-

a)Author to whom correspondence should be addressed.

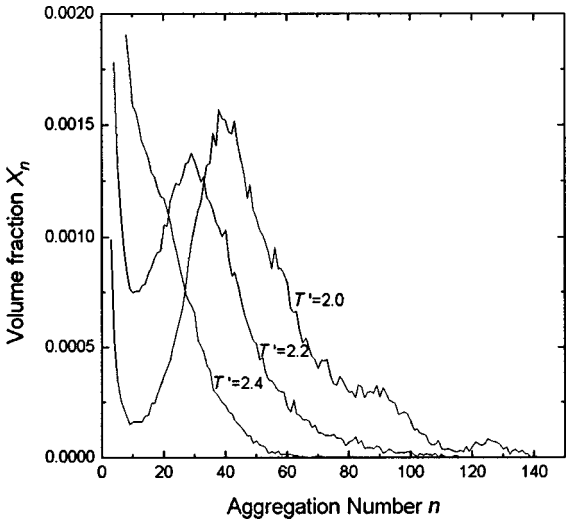

FIG. 1. Variation of the micellar size distribution with scaled temperature T' (interaction strength) in a small $20\times20\times20$ system with a surfactant volume fraction of 7.5%. Finite size effects are apparent in the $T'=2.0$ distribution (see the text).

gregation. The average of this distribution therefore corresponds to the weight average aggregation number of the aggregates.

At the highest temperature $T'=2.4$ there is a slight shoulder in the size distribution at an aggregation number of about 20, indicating that micelles are just barely stable at this temperature. For the H_2T_2 surfactants used here, this scaled temperature corresponds to a value of $n_T\chi=10$, where n_T is the number of tail beads. Previous studies[3] using surfactants of different sizes at fixed χ found that micelles did not form at $n_T\chi=8$, while micelles did form at $n_T\chi=12$ or higher.

As the temperature is lowered to $T'=2.2$, a well-defined peak occurs in the size distribution, indicating separation of the surfactant population into micelles and isolated surfactants or premicelles. As the temperature is lowered further to $T'=2.0(n_T\chi=12)$, the separation between premicelles and true micelles becomes more distinct, as exemplified by the deepening of the minimum in the distribution at an aggregation number of about 10. At this temperature the distribution becomes more polydisperse as the fraction of surfactant in larger aggregates increases. This temperature of $T'=2.0$ was chosen for the large simulation. Lowering the temperature further to obtain an even greater separation slows down the simulation dramatically. This slowing down is because the rate of desorption of a monomer from a micelle is a thermally activated process governed by the desorption energy.

The $T'=2.0$ distribution has three peaks at aggregation numbers of about 40, 90 and 125. One possible configuration of the $20\times20\times20$ system consists of three aggregates of roughly equal size (ca. 40) in equilibrium with the 25 surfactants with an aggregation number of less than 10 (i.e., the monomers and premicelles). The small but well-defined peak at an aggregation number of about 125 corresponds to configurations of the system wherein a single micelle of aggregation number ca. 125 is in equilibrium with the remaining 25 nonmicellar surfactants. Micelles larger than this size are unable to form due to the finite-size of this small simulated system. As we demonstrate below, the peaks at 90 and 125 are due to the small size of the system, and they disappear in the larger simulations.

EQUILIBRATION

The main simulation run was conducted on a $60\times60\times60$ lattice with a volume fraction of 7.5% surfactant as before. The simulation was equilibrated for 2.7×10^{10} Monte Carlo steps, or 1.67×10^6 Monte Carlo steps per surfactant bead (MCS/B). The temperature during this time was held constant at $T'=2.0$. It was observed[17] that the configurational energy of the system reached its equilibrium value approximately three times faster than did the average aggregation number. Hence, we used the time development of the average aggregation number to determine when the micelles had grown to their equilibrium size. The conformational energy is not as sensitive to the form of the size distribution, as there is only a relatively small conformational energy difference between two moderately large aggregates, and the larger aggregate which they may form by coalescence.

CORRELATIONS AT EQUILIBRIUM

Once we have determined that the system is at equilibrium, there remains the question of how long it takes the system to evolve from a given configuration to a statistically independent configuration. An estimate of this time is required to determine how long the simulation must run to sample the complete size distribution representatively. An estimate of this time can be obtained from the autocorrelation function for the aggregation number of a surfactant

$$\rho_{aa}(t)=\frac{\langle a(t)a(t'+t)\rangle-\langle a\rangle^2}{\langle a^2\rangle-\langle a\rangle^2},$$

where $a(t)$ is the aggregation number of a surfactant at time t (in MCS/B) and the average is over all surfactants and all times t'. A semilog plot of $\rho_{aa}(t)$ vs time t (not shown) has a long-time linear portion for $t>30\,000$ MCS/B. The slope of this portion can be used to determine a characteristic time, τ_{aa}, for the single surfactant-aggregate autocorrelation function. During this time period ρ_{aa} is proportional to $\exp(-t/\tau_{aa})$. The value obtained for τ_{aa} was found to be 23 900 MCS/B. This time can be related to the rate at which monomers desorb from a micelle.[17]

The requirements for obtaining a ''smooth'' distribution relate to the size of the system and the value for τ_{aa}. An order of magnitude estimate for the time required to obtain a smooth distribution can be obtained by considering the fluctuations in the size of a given micelle. A time averaged size distribution of a micelle can be expected to be a Gaussian distribution for short times, centered on the initial size. The width of this peak will increase with time in a manner similar to a diffusive process so that the time required for the width of the distribution (as measured by the standard deviation of the Gaussian) to reach a value of σ will require a time proportional to $\sigma^2\tau_{aa}$. The time required for the distribution to become smooth is that required for the peaks from separate

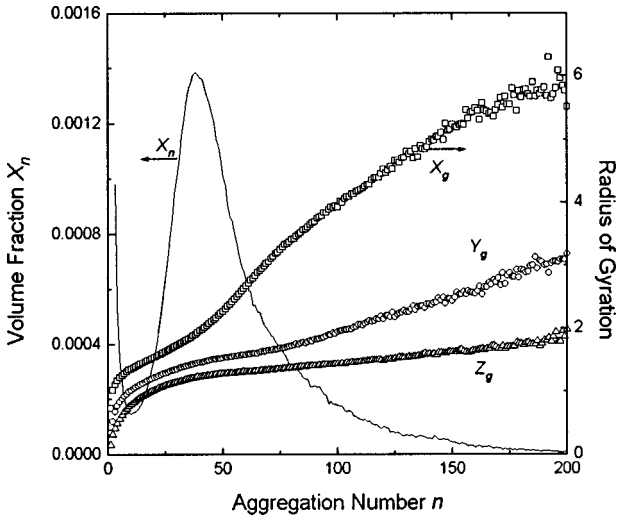

FIG. 2. Micellar size and shape distributions in a larger $60\times60\times60$ system at $T'=2.0$ with a surfactant volume fraction of 7.5%. X_g, Y_g, and Z_g are the ordered components of the radius of gyration tensor for aggregates of size n.

micelles to overlap. For the peaks to overlap, σ^2 needs to be made proportional to $\langle a^2\rangle/N_{\mathrm{mic}}$, which is a measure of the mean-square distance between single micelle peaks in the distribution. N_{mic} is the average number of micelles in the system, which can be estimated as $N_s/\langle a\rangle$, where N_s is the number of surfactant molecules in the system.

Hence, the time required to obtain a smooth distribution can be estimated as

$$\tau_{\mathrm{dist}}\sim\frac{\langle a\rangle\langle a^2\rangle\tau_{aa}}{N_s}.$$

Using this relation, $\tau_{\mathrm{dist}}=1\times10^6$ MCS/B for the large simulation. The smoothness of the distribution in Fig. 2 can be attributed to the length of the simulation being significantly larger than τ_{dist}.

MICELLAR SIZE AND SHAPE DISTRIBUTIONS

After the equilibration period, the properties of interest were averaged over a period of 4.583×10^6 MCS/B (c.f. τ_{dist} calculated above). Over this time the system was sampled 11 000 times at regular intervals. The equilibrium size distribution for the $60\times60\times60$ lattice system shown in Fig. 2 is similar to that shown in Fig. 1 for the $20\times20\times20$ lattice at the same temperature and concentration. However, the secondary peaks in the size distribution at aggregation numbers of about 90 and 125 (Fig. 1) have now disappeared, confirming that these peaks were artifacts of small system size. The system contains 4050 surfactants and ca. 70 aggregates. The distribution is smooth and has a single peak at an aggregation number of about 40 with a long tail to higher aggregation numbers. This type of distribution is considered to be in qualitative agreement with experiment,[8,19,20] and recent lattice simulations.[9] However, recent off-lattice simulations of a similar surfactant did not produce a significant number of aggregates with aggregation numbers larger than ca. 50.[15]

To investigate the structure of the micelles the radius of gyration tensor was calculated for the aggregates and diagonalized into the form

$$R_g^2=\begin{pmatrix}X_g^2&0&0\\0&Y_g^2&0\\0&0&Z_g^2\end{pmatrix},$$

where the diagonal elements are ordered so that $X_g>Y_g>Z_g$. This transformation is a rotation of the micelle so that the principal axes of the radius of gyration tensor coincide with the (Cartesian) coordinates axes, and X_g^2, Y_g^2, and Z_g^2 are the ordered eigenvalues of the mean-square radius of gyration tensor. These values characterize the size of the micelles in each of the principal directions. The root mean square values of the radius of gyration tensor are shown in Fig. 2.

For comparison, note that for a cylinder of length $2L$ and radius R, Y_g and Z_g are equal to each other and proportional to R, and X_g is proportional to L. The simulation data are consistent with the observation that the peak in the distribution centered at an aggregation number of ca. 40 is comprised of ''spherical'' micelles. (The instantaneous shapes of the micelles are not perfectly spherical, and the inequality of the three principle components of the radius of gyration tensor is maintained by the ordered averaging.)

In the size range from 40–80 the micelles grow in one direction to form spherically capped cylinders, with approximately the same minimum dimension as the 40 spheres. As the micelles grow longer, the cylinders become flexible and X_g falls below the linear form expected for rigid cylinders. This flexibility also explains why Y_g and Z_g increase from the constant value expected for rigid cylinders as the micelles become more wormlike. These observations were also confirmed by visualization and inspection of snapshots of the system (e.g., see Fig. 5).

The size distributions were fitted to simple theories which assume the micelles are spherical and cylindrical (for example, see Israelachvili[21]). The aggregate distribution is split into two components

$$C_N=C_N^S+C_N^C,$$

where C_N^S is the volume fraction of surfactants in spherical micelles of aggregation number N and C_N^C is the volume fraction of surfactants in cylindrical micelles of aggregation number N.

The main peak in the distribution is fitted to a Gaussian distribution which is expected from a simple model[21] for spherical micelles

$$C_N^S=C_M\exp\left(\frac{-(N-M)^2}{2\sigma^2}\right),$$

where M is the most probable aggregation number for the spherical micelles with peak height C_M and σ is the width of the Gaussian distribution.

The long tail in the distribution is fitted to an exponential distribution[21] for cylindrical micelles of the form

$$C_N^C=\beta\exp(-\alpha N)f(N)$$

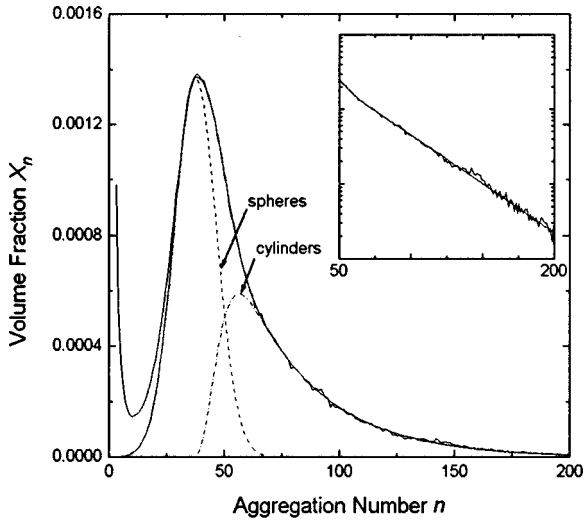

FIG. 3. Micellar size distribution fitted to the forms expected for spherical and cylindrical micelles in the 7.5% surfactant volume fraction simulation. Inset is the size distribution in the range $n=50$ to $n=200$ on a semi-log plot to show the exponential tail of the cylindrical micelles.

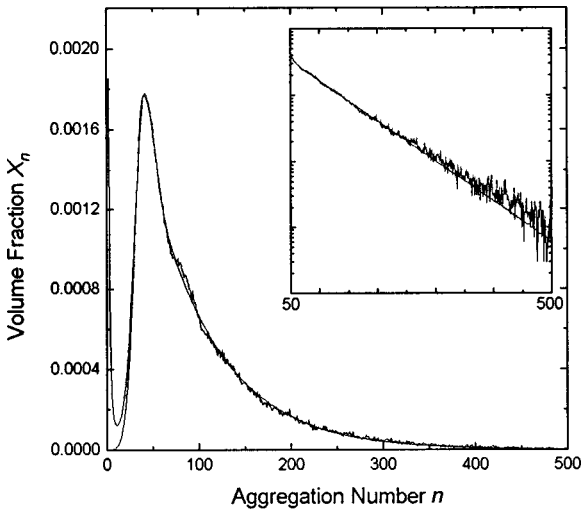

FIG. 4. Micellar size distribution fitted to the forms expected for spherical and cylindrical micelles in the 15% surfactant volume fraction simulation. Inset is the size distribution in the range $n=50$ to $n=500$ on a semilog plot to show the exponential tail of the cylindrical micelles.

where $f(N)$ is a matching function of the form

$$f(N)=\begin{cases} 0 & N\leqslant M \\ \dfrac{C_M-C_N^S}{C_M} & N>M \end{cases}.$$

The matching function has a value of unity at large aggregation numbers and smoothly takes the cylindrical micelle distribution to zero at an aggregation number of M. At values lower than M there can be no cylindrical micelles by definition.

Figure 3 shows the fit to the data from the 7.5% surfactant volume fraction simulation. For $n<40$ the fitted distribution is comprised entirely of spherical micelles. In the range $n=40$ to $n=70$ the distribution is a mixture of spherical and cylindrical micelles. For $n>70$ the fitted distribution is due solely to cylindrical micelles. The inset to Fig. 3 shows the micelle distribution for n in the range from 50 to 200 on a semilog plot. The linear region for $n>70$ on the semilog plot corresponds to the exponential distribution for cylindrical micelles. The simple model used here assumes that the distribution is comprised entirely of fully formed micelles and monomers only. This does not account for the premicelles in the aggregation range $n=2$ to $n=40$, which are not well-developed spheres.

Another simulation at a surfactant volume fraction of

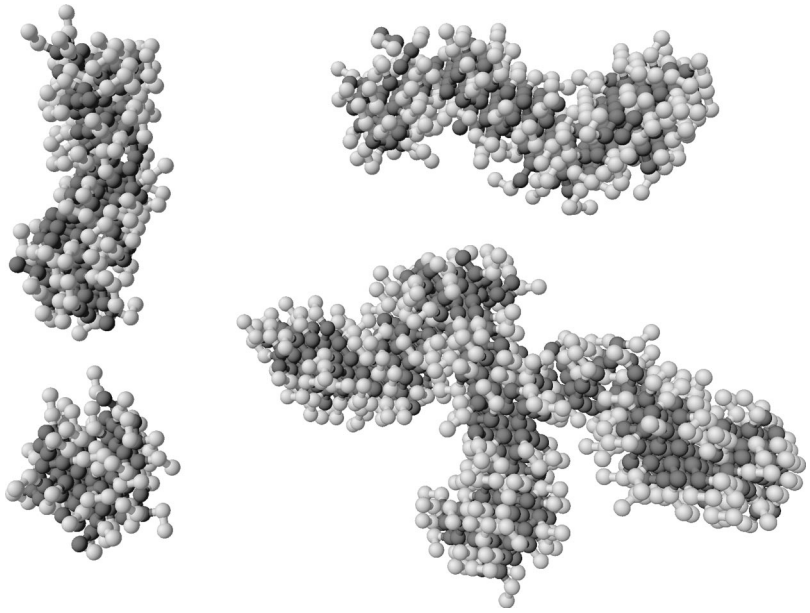

FIG. 5. Micelles taken from a single snapshot of the 15% surfactant volume simulation. They have aggregation numbers of 42, 91, 125, and 269 (starting at the lower left and proceeding clockwise).

15% was also performed on a $60\times60\times60$ lattice. The results were fitted to the same aggregate model and the result is shown in Fig. 4. Once again the distribution fits the cylindrical micelle model for $n>70$ (see inset). As the surfactant concentration is increased the distribution becomes broader, with the excess surfactant moving into the long cylindrical tail of the distribution. A number of micelles were extracted from this system and are shown in Fig. 5. These micelles were oriented to have their two largest dimensions in the plane of the page. As can be seen, the larger micelles are not simply colliding spherical micelles but are fully developed flexible wormlike micelles that may have one or more branch points. The $n=269$ micelle has a single branch point and was the largest aggregate at the time the snapshot was taken. The fact that the larger aggregates are not exactly the rigid cylinders assumed in the theory does not appear to affect the fits in Figs. 3 and 4 significantly. The semilog plots confirm the expected exponential decay to a good approximation.

CONCLUSION

Equilibration of simulated micellar systems is better monitored using the average aggregate size rather than the configurational energy of the system. The surfactant aggregate autocorrelation function can be used to estimate how long a simulation must be run to sample the equilibrium configuration space of the system representatively. Thermodynamic models of micelles usually assume that the micelles have a well defined geometric shape. Our results confirm this assumption for self-assembled micellar aggregates, whose size distributions are found to be consistent with the simple thermodynamic models for micelles of spherical and cylindrical shape in equilibrium with each other.

[1] R. G. Larson, J. Chem. Phys. **89**, 1642 (1988).
[2] R. G. Larson, J. Chem. Phys. **91**, 2479 (1989).
[3] R. G. Larson, J. Chem. Phys. **96**, 7904 (1992).
[4] R. G. Larson, Macromolecules **27**, 4198 (1994).
[5] D. Stauffer, N. Jan, Y. He, R. B. Pandey, D. P. Marangoni, and T. Palmer, J. Chem. Phys. **100**, 6934 (1994).
[6] A. T. Bernardes, Vera B. Henriques, and P. M. Bisch, J. Chem. Phys. **101**, 645 (1994).
[7] C. M. Wijmans and P. Linse, Langmuir **11**, 3748 (1995).
[8] A. D. Mackie, K. Onur, and A. Z. Panagiotopoulos, J. Chem. Phys. **104**, 3718 (1996).
[9] J.-C. Desplat and C. M. Care, Mol. Phys. **87**, 441 (1996).
[10] B. Smit, P. A. J. Hilbers, K. Esselink, L. A. M. Rupert, and N. M. van Os, J. Phys. Chem. **95**, 6361 (1991).
[11] B. Smit, K. Esselink, P. A. J. Hilbers, N. M. van Os, L. A. M. Rupert, and I. Szleifer, Langmuir **9**, 9 (1993).
[12] S. Karaborni, N. M. van Os, K. Esselink, P. A. J. Hilbers, Langmuir **9**, 1175 (1993).
[13] S. Karaborni, K. Esselink, P. A. J. Hilbers, B. Smit, J. Karthauser, N. M. van Os, and R. Zana, Science **226**, 254 (1994).
[14] D. R. Rector, F. van Swol, and J. R. Henderson, Mol. Phys. **82**, 1009 (1994).
[15] F. K. von Gottberg, K. A. Smith, and T. A. Hatton, J. Chem. Phys. **106**, 9850 (1997).
[16] P. J. Flory, *Principles of Polymer Chemistry* (Cornell University Press, Ithaca, New York, 1954).
[17] P. H. Nelson, Doctoral thesis, Department of Chemical Engineering, Massachusetts Institute of Technology (in preparation).
[18] P. H. Nelson, T. A. Hatton, G. C. Rutledge, J. Chem. Phys. **107**, 1269 (1997), and references therein.
[19] H. Wennerström and B. Lindmann, Phys. Rep. **52**, 1 (1979).
[20] M. He, R. M. Hill, Z. Lin, L. E. Scriven, and H. T. Davis, J. Chem. Phys. **97**, 8820 (1993).
[21] J. Israelachvili, *Intermolecular and Surface Forces*, 2nd ed. (Academic, London, 1991).